ACCOUNTS of chemical research

Article

pubs.acs.org/accounts

Characterization of Ligand Shell for Mixed-Ligand Coated Gold Nanoparticles

Quy Ong,[†] Zhi Luo,[†] and Francesco Stellacci*

Institute of Materials, Ecole Polytechnique Fédérale de Lausanne (EPFL), Lausanne-1015, Switzerland

CONSPECTUS: Gold nanoparticles owe a large number of their properties to their ligand shell. Indeed, many researchers routinely use mixtures of ligand molecules for their nanoparticles to impart complex property sets. It has been shown that the morphology of ligand shells (e.g., Janus, random, stripelike) leads to specific properties. Examples include wettability, solubility, protein nonspecific adsorption, cell penetration, catalysis, and cation-capturing abilities. Yet, it remains a great challenge to evaluate such morphologies in even the most fundamental terms such as dimension and shape. In this Account, we review recent progress in characterization techniques applicable to gold nanoparticles with ligand shells composed of mixed ligands. We divide the characterization into three major categories, namely, microscopy, spectroscopy, and simulation. In microscopy, we review progresses in scanning tunneling microscopy (STM), atomic force microscopy (AFM), and scanning/transmission electron microscopy. In spectroscopy, we mainly highlight recent achievements in nuclear magnetic resonance (NMR), mass spectrometry (MS), small angle neutron scattering (SANS), electron spin resonance (EPR), and adsorption based spectroscopies. In simulation, we point out the latest results in understanding thermodynamic stability of ligand shell morphology and emphasize the role of computer simulation for helping interpretation of experimental data. We conclude with a perspective of future development.

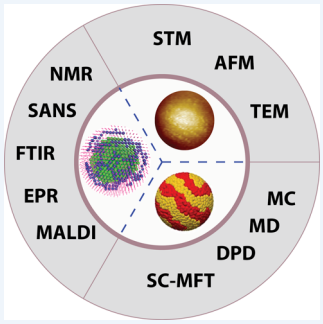

1. INTRODUCTION

Within this Account, gold nanoparticles (NPs) are defined as a metallic gold core covered by a monolayer of organic molecules (typically thiolated compounds) that we call ligands. The gold core has the diameter of several nanometers, and the ligand molecules are attached to the gold surface via S−Au bonds. This core−shell construct can be made by many facile and robust synthetic techniques.[1] They can be generally categorized into two widely adopted methodologies: direct synthesis in the presence of thiols, and postsynthesis functionalization by ligand exchange. Both the NPs' core and the ligand shell are important in determining the NPs' properties.[2] Notably, diverse functionalities of gold NPs can be achieved through tuning ligand molecules, an advantage that allows the NPs to be tailor-made for specific applications. Many applications of gold NPs can be found in electronics, drug delivery, catalysis, and sensing.[2,3] Furthermore, the structure of the ligand shell and of the core can also be synergistically designed and exploited, which very often leads to the nonadditive nature of NP properties and could be crucial for many applications.[4]

Both the ligand−shell composition and its structure have been shown to contribute significantly to the chemical, biological, and interfacial behaviors of gold NPs. Increasing evidence in the literature has pointed to effects of the morphology of the ligand shell on determining particles' properties such as wettability,[5] solubility,[6] protein nonspecific adsorption,[7,8] cell penetration,[9] catalysis,[10] and cation capturing abilities.[11] As a consequence, the key step in nanoparticle characterization has to be the determination of the ligand shell morphology. Hereafter, we use the term morphology to refer to the structure of molecular domains in the mixed ligand shell.

In this Account, we attempt to highlight recent development in characterization techniques of the ligand shell of gold NPs, specifically focusing on techniques that help elucidate the structure of ligand shells composed of binary monolayers. The techniques are grouped in three major categories: microscopy, spectroscopy, and simulation. All the strengths and major achievements of the techniques are discussed in their respective sections. The key shortcomings are discussed in the perspectives section and used as a point of departure to suggest toward where the field should be moving in the future.

2. MICROSCOPY

Due to the size of the gold cores and the small dimensions of ligand shell domains, not many microscopic tools are available for direct visualization of ligand structures. So far, scanning probe techniques such as scanning tunneling microscopy (STM) and atomic force microscopy (AFM) have been the main suitable microscopy techniques. STM uses as a feedback the tunneling current between a sharp metallic tip and a substrate. Imaging gold NPs greatly benefits from the resolution this technique can provide. Once the particles are clean from free ligands and are attached firmly to a conductive flat surface such as Au(111) or HOPG, the ligand shell morphology can be resolved based on the conductivity and height difference of the molecular component of the ligand shell. Here, we emphasize that any attempt to image gold NPs by STM has to consider three important issues. The first is the

Received: April 4, 2017
Published: August 3, 2017

DOI: 10.1021/acs.accounts.7b00165
Acc. Chem. Res. 2017, 50, 1911−1919

cleanliness of gold NPs. The particles must be as free from organic residues (such as the unattached ligands) as possible. This requirement is crucial because the unattached ligands can easily contaminate the scanning tip, quickly degrading its ability to produce good images. In our experience, a necessary condition for particles to be image-able is that their H^1 NMR spectrum is free from sharp peaks (subsection 3.1). The second issue is that gold NPs must be anchored firmly onto the surface. The anchoring is needed to avoid the particle movement and/or vibrations when the tip traverses across the surface. Even a small movement of the NPs will compromise the resolution of the image. The latter condition can be circumvented when imaging in vacuum at low temperature, or in the rare cases when a particle adheres to a crevice on the surface. In order to routinely achieve substrates that meet ideal imaging conditions, typically we prepare a thiolated self-assembled monolayer (SAM) on Au(111) on a mica substrate. The SAM is composed of a short "filler" molecule (butanethiol) and an anchoring dithiol molecule considerably longer (e.g., 1,16-hexadecane dithiol). On such a substrate we deposit a monolayer of NPs by either the Langmuir-Schaeffer approach or by drop-casting a dilute dispersion of NPs. The third issue is to achieve a single NP layer as imaging through thick NP films is challenging. We have managed to image bilayers and occasionally thicker layers but all our best images are from single layers, Figure 1.

Taking advantage of high topographical resolution achievable by STM, in 2004, our group showed the existence of nanodomains that resembled ripples or stripelike domains on gold NP coated with a binary mixture of ligands.[8] For instance, STM images of gold NPs coated with octanethiol and mercaptoproprionic acid OT/MPA (2:1) present stripelike domains with ∼1 nm thickness. Caution has to be exercised when acquiring and interpreting images of striped NPs as these STM images bear similarities to feedback loop artifacts if the imaging gains are not set properly.[14,15] Visually, the latter appear as parallel or wavy lines. It was shown[16−18] that, to differentiate the features due to true tip−sample interactions from feedback loop artifacts, one needs to produce various images at different tip velocities and show that the features are invariant. It was demonstrated that, in plots of the average spacing of the features as a function of tip velocity, feedback loop artifacts are characterized by a linear trend that passes through the origin; while the plots of stripelike domains are characterized by lines that are close to being horizontal.[18,19] For imaging NPs, scanning the same area at different angles can provide an additional verification of real stripelike features against the feedback loop artifacts.[12] This latter control can be challenging as stripelike domains reveal complexity (e.g., variation in thickness and local defects) that renders the interpretation of the images at different angles complex.

Due to such high complexity, quantitative measurements can be tedious and the quantification of stripe dimension can be subject to operator's bias. Biscarini et al. developed a fast and powerful technique based on power spectral density (PSD) to extract correlation lengths from STM images of NPs.[20] PSD of an STM image is its norm squared fast Fourier transform (FFT), and it represents the contribution, i.e. power, of different length scales displayed in the frequency domain of the image. A PSD curve of a representative STM image of NP can be usually decomposed to three segments as shown in Figure 2a. As illustrated in the figure, characteristic features of the curve depend on the particle size and on the distribution (in size and orientation) of the stripelike domains. Due to its

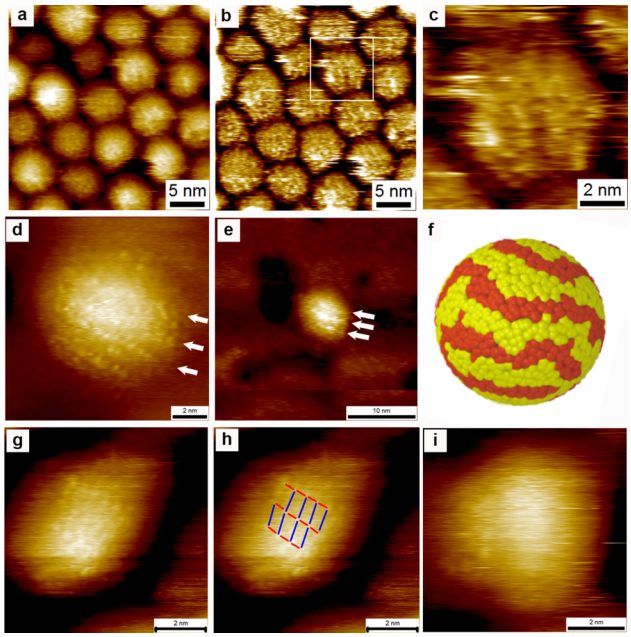

Figure 1. STM images of mixed ligand coated NPs showing stripelike features of the ligand shell. (a) STM topography image of gold NPs coated with dodecanethiol and hexanethiol; the image was recorded in phenyloctane. (b) STM topography of image (a) after the low frequency contribution is removed to show the crispness of the domains. (c) Enlargement of one particle in image (b). (d) Molecular resolution STM topography image of a gold NP coated with mercaptoproprionic acid and octanethiol. (e) Low resolution image of this particle showing that the stripes are smooth and appear uniform. (f) Coarse grain simulation model of a nanoparticle showing stripelike domains. Red and yellow beads represent two dislike molecules; for example, short and long molecules, respectively. (g) High resolution STM image of a gold NP coated with 11-mercapto-1-undecanol (C11OL) and 4-mercapto-1-butanol (C4OL). (h) Same image presented in (g) with blue dashes having a dimension of 1 nm, and red dashes of 0.5 nm to guide visualization of stripes. (i) STM image of a gold NP coated with C11OL and C4OL showing the Janus structure. Reproduced with permission from refs 12 and 13. Copyright 2014 Royal Society of Chemistry and 2013 American Chemical Society.

quantitative nature, this PSD-based method can also be conveniently used to judge differences between samples in a straightforward manner. For example, if the shoulder is located at a higher spatial frequency, the average size of the features on gold NP is smaller. A whole PSD curve could also be fit with a phenomenological functional from which quantitative measurements of particle size and domain features can be extracted. Biscarini et al. showed that by using this PSD technique, STM images from different laboratories, different scales, or different scanning conditions can be analyzed efficiently, and reported that striped features with a correlation length of ∼1 nm could be cross-checked and indeed confirmed.[20] The correlation length of ∼0.5 nm on the other hand is measured in homoligand coated gold NPs. PSD estimation can be easily computerized and enables analysis of a large amount of images in short period of time. Lately, Ong et al. imaged stripelike domains both in air and in solvent to attempt to evaluate the consistency of the imaging.[21] Indeed, large data sets were acquired and PSD analysis helped to show that equivalent spatial frequency is present in both cases, as shown in Figure 2b.

DOI: 10.1021/acs.accounts.7b00165
Acc. Chem. Res. 2017, 50, 1911−1919

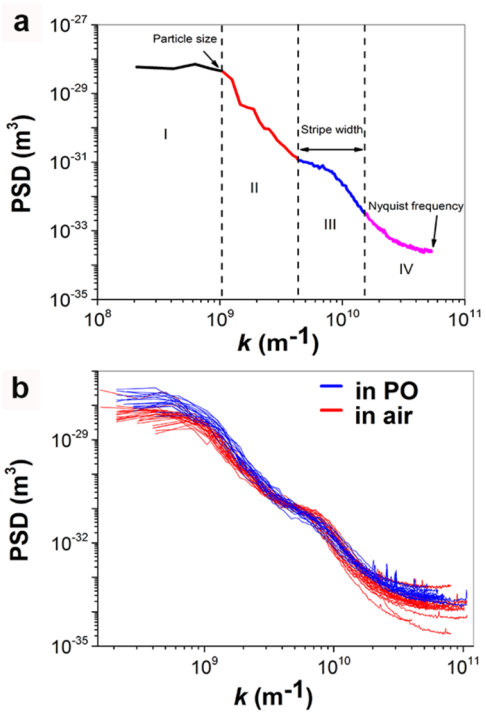

Figure 2. (a) Representative PSD curve of an STM image containing striped NPs. The curve has been split into regions that have been colored differently in order to facilitate the explanation of its meaning. The PSD curve is the norm squared fast Fourier transform (FFT) averaged for horizontal direction, representing the contribution, i.e., power, of different length scales displayed in the frequency domain of the image. A PSD curve of an STM image of gold NP is usually examined at four segments: (I) plateau at low frequency (black segment) that stop at the frequency from which the particle size can be estimated, (II) a decay that is related to the particle curvature and the characteristic $1/f$ noise of the microscope (blue segment), (III) a broad shoulder or peak at high frequency that contains the length scale of the features on the surface of gold NP (red segment), and (IV) a flat part that ends at the Nyquist frequency which indicates length scales that lack content in the image (violet segment). (b) Comparative study of STM images recorded from gold NP coated with 1-nonanethiol (NT) and 4-methylbenzenethiol (MBT). The imaging was performed in air (red) or with the particle substrate and STM tip submerged in phenyloctane (blue). The overlap of the curves demonstrates a consistency in the correlation of length of the stripelike domains. Reproduced with permission from ref 21. Copyright 2014 Royal Society of Chemistry.

Stripelike domains have also been imaged on the surface of binary-coated gold NPs (hexanethiol−dodecanethiol) when they were completely submerged in a high-boiling-point solvent such as phenyloctane. Such clear images of the stripelike domains have been acquired due to the fact that the phenyloctane maintains a clean environment during image recording, and partially solvates the hydrophobic ligand molecules.[12]

High-resolution images of the ligand shell of gold NPs coated with a binary mixture, in which positions of individual thiols are molecularly resolved, have been acquired only recently, Figure 1g and d.[13] Figure 1g shows an STM image of a single nanoparticle coated with 11-hydroxyl-undecanethiol and 4-hydroxyl-butanethiol C11OL/C4OL (1:1). Single C11OL molecules are imaged on the nanoparticle and appear as dots. The dots align in two stripes with a spacing of ∼0.5 nm along and ∼1 nm across the stripes.

AFM has also shown a capacity to resolve the structure of the ligand shell when operating in liquid, in small-amplitude mode. Molecular resolution images, equivalent to STM images, of stripelike domains on gold NP covered with 1-octanethiol and 6-mercaptohexan-1-ol (MHol) could be obtained using this technique.[5]

Scanning/transmission electron microscopy (S/TEM) is a versatile physical characterization tool for NPs. It is mostly used for obtaining shape, and size distribution and elemental composition of NP cores. The organic ligand shell is often invisible under the electron beam. The use of monolayer graphene as a supporting film and low acceleration voltage (80 KV) in an aberration-corrected TEM has allowed direct visualization of the ligand shell of the citrate-coated gold NPs as demonstrated in a seminal work by Lee et al.[23] Discerning different ligand molecules and ligand shell morphology remains an open challenge for this technique.

Yang et al. used osmium tetroxide as a staining agent to help image the ligand shell of gold NPs (tens of nm in size) functionalized with mixed lipid layers that form patchy domains by molecular phase separation.[24] Some ligands (e.g., metal oxide cluster α-$AlW_{11}O_{39}^{9-}$) that have strong contrast for cryo-TEM can be used for direct imaging (Figure 3). This and other approaches are useful but limited to large particles.[25]

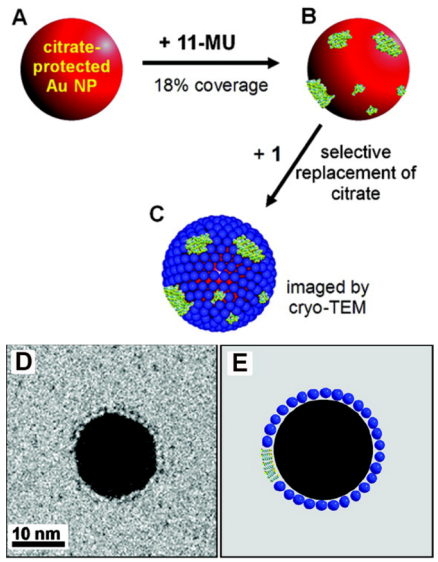

Figure 3. Presence of molecular patchy domains on a gold nanoparticle revealed by the use of α-$AlW_{11}O_{39}^{9-}$ (**1**) and cryo-TEM. The mixed ligand shell in particle (B) is made by partial replacement of citrate on a citrate coated gold NP (particle (A)) with mercapto-undecacarboxylate (**11-MU**) followed by substituting the leftover citrate on (B) with the cluster 1 to form (C) for imaging. (D) Cryo-TEM image of the particle (C). (E) Illustration of the 2D projection of the particle (C). Reproduced with permission from ref 22. Copyright 2012 American Chemical Society.

3. SPECTROSCOPY

Contrary to microscopic techniques, spectroscopic techniques normally provide ensemble characteristics of a whole nanoparticle sample. Several spectroscopic techniques have been successfully applied to obtain structural information on the ligand shell in mixed monolayer coated gold NPs. In this section, we mainly showcase recently developed techniques that have potentials for a broad range of NPs.

DOI: 10.1021/acs.accounts.7b00165
Acc. Chem. Res. 2017, 50, 1911−1919

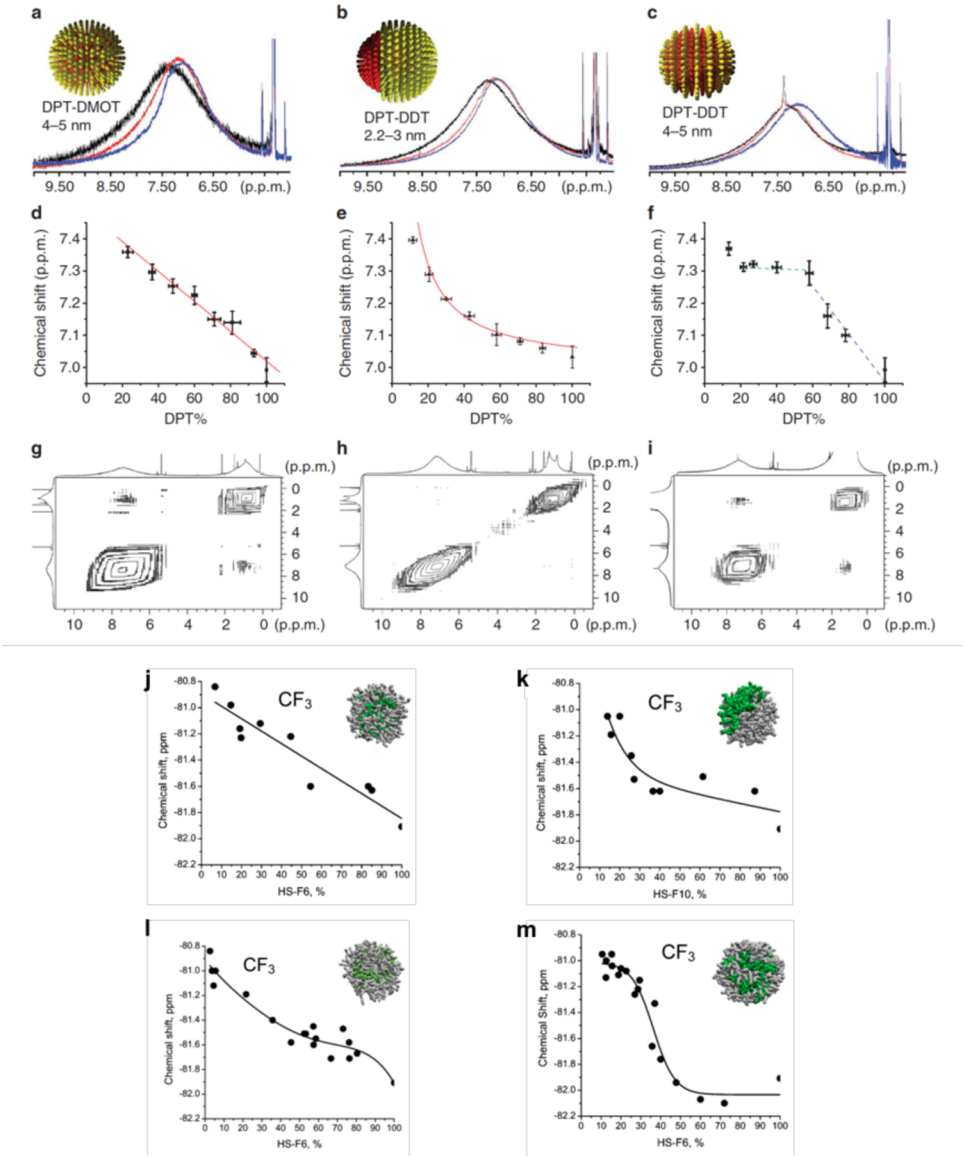

Figure 4. NMR of mixed ligand protected nanoparticle. ^{1}H NMR (a–c) and chemical shifts (d–f) and NOESY (g–i) of randomly mixed, Janus and patchy NPs, respectively. (j–m) ^{19}F NMR and DPD simulation of mixed hydrocarbon and fluorinated ligand protected nanoparticle of various morphologies, i.e., random (j), Janus type (k), and stripelike (l,m). Reproduced with permission from refs 27 and 28. Copyright 2012 Nature Publishing Group and 2016 American Chemical Society.

3.1. NMR

NMR is a powerful technique for the characterization of NPs, and we refer to an excellent review by Marbella and Millstone for a comprehensive overview.[26] Briefly, line broadening of resonance peaks is usually observed in nanoparticle NMR, and it can be used as a gauge for the absence of unbound molecules. The ligand ratio on NP surfaces can be determined after proper etching of the metal cores to release ligands from NP surfaces.

For complex ligand shells such as those of mixed ligand protected NPs, the chemical shifts and line broadening effects are influenced by the neighboring ligand species. We have exploited the sensitivity of ^{1}H NMR measurements to study various types of mixed ligand shell structures.[27] The upfield shift of aromatic ligands was used as an indication of the neighboring environment of the ligands. For random mixtures, the ligand's chemical shift shows a linear dependence on the shell composition due to equivalence between the global and local composition. For Janus morphologies, the shift is proportional to the inverse of the composition, as it was shown analytically.[27] For patchy particles, the situation becomes more complex and the trend depends on the evolution of the shape of phase separation domains. Cross-peaks in 2D nuclear Overhauser effect spectroscopy (NOESY) can only be observed when the nuclear spins are close enough (<0.5 nm). Therefore, the absence of cross-peaks can distinguish Janus particles from other types of morphologies. Recently, ^{19}F NMR was exploited to study the morphology of mixed ligand NPs coated with hydrocarbon and fluorinated ligands.[28] The trends determined by the chemical shifts of a random, patchy/striped and Janus NP were found to be consistent with the NOESY experiments and dissipative particle dynamics (DPD) simulations, Figure 4. For random and Janus types of NPs, the ^{1}H NMR and ^{19}F NMR results show almost the same trend. The trends for stripe/patchy NPs show the expected sigmoid behavior but differ somewhat on the specific shape of the curves. This is expected as the shape depends on

DOI: 10.1021/acs.accounts.7b00165
Acc. Chem. Res. 2017, 50, 1911–1919

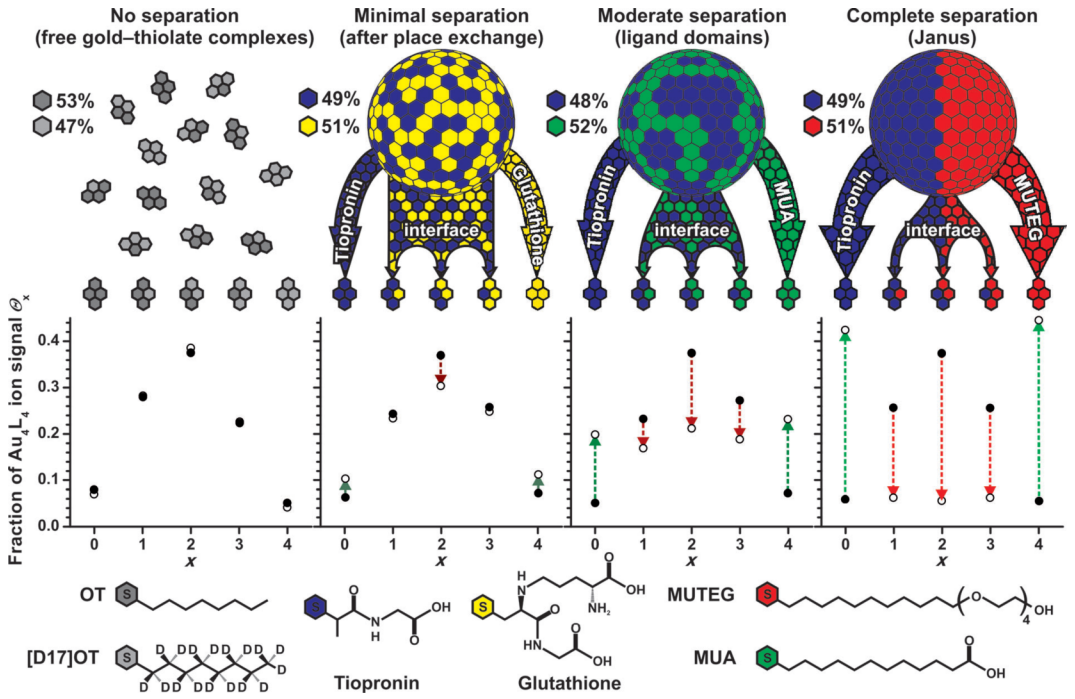

Figure 5. MALDI-MS investigation of molecular phase separation in mixed ligand coated NPs. Among the fragments of Au-thiol complexes caused by the MALDI process, only the Au_4L_4 ion species are analyzed since they are the most abundant fragments. For a binary ligand coated gold NP, 5 combinations of Au_4L_4 will be found and they are labeled from 0 to 4 in the *x*-axis of the plots. In other words, if the ligand shell contains a binary mixture of thiols A and B, the 5 species of the Au_4L_4 complexes analyzed are $Au_4A_{4-x}B_x$ (x = 0, 1, 2, 3, 4). Their corresponding abundances obtained experimentally from 4 different types of mixed ligand coated gold NPs are illustrated by open circles. The binomial distribution, which corresponds to random morphology, is presented by filled black dots. The deviations from the binomial distribution, represented by an arrow for each species, indicate the presence of molecular phase separation in the ligand shell that ranges from completely mixed, to patchy domains, and to the Janus structure. The ligand shell compositions of the 4 investigated particles are octanethiol (OT)/deuterated OT, tiopronin/glutathione, 11-mercaptoundecanoic (MUA)/glutathione, tiopronin/mercaptoundecyltetraethylene glycol (MUTEG), respectively. Reproduced with permission from ref 35. Copyright 2011 Wiley-VCH.

many parameters of the stripelike domains including the thickness.[27]

As successful example studies of NP systems combining 1D and 2D NMR techniques, the works described above still have certain limitations, such as the choice of ligands (to observe the cross-peaks) and the requirement of the tenability of the ligand shell composition. However, it demonstrates the possibility of studying complex ligand shell structures by using a library of NMR techniques. The limitations could be overcome by measuring nuclei whose chemical shift is more sensitive and with a broader range, such as ^{13}C NMR. More detailed structural and dynamic information on mixed ligand protected gold NPs could be obtained by applying other advanced NMR techniques and by combining them with various simulation methods. It has been shown that using paramagnetic lanthanide labels, it is possible to access detailed distribution of mixed ligands and distances among those labels.[29] There are also some encouraging examples of the structural characterization of model nanoparticle systems such gold nanoclusters using a variety of 2D NMR techniques.[30]

3.2. FTIR

FTIR has been widely applied to study NPs.[31] It allows one to obtain molecular composition, and it is sensitive to molecular conformation and local chemical environment, e.g., frequency of CH_2 stretching is influenced by intramolecular conformation disorder. Using very similar arguments to the ones discussed for NMR shift, we used FTIR shifts to determine phase separation of mixed ligand shells on gold nanoparticle surfaces.[32]

3.3. SANS

Small angle neutron scattering (SANS) is also a powerful technique to probe structural information on the ligand shell as the scattering cross section of neutron does not depend on the atomic number but vary with isotopes. In ref 12, SANS spectra were recorded for two identical NPs differing only in the deuteration of one of the molecules in the ligand shell. The first particle was coated with perdeuterated dodecanethiol and hexanethiol, and the other with dodecanethiol and perdeuterated hexanethiol. The spectra were then fitted simultaneously using the simulated annealing approach implemented in MONSA program, which results in a reconstructed ligand-shell−gold-core 3D model of the particle.

3.4. Mass Spectrometry

Mass spectrometry has been used to characterize NPs, for example, to determine their molecular weight.[33] As for mixed ligand NPs, it has been demonstrated that the identity and ligand ratio could be determined by the LDI-MS technique.[34] An interesting work was reported by Harkness et al., in which matrix assisted laser desorption/ionization (MALDI) was used to examine the phase separation behavior of various mixed ligand protected NPs.[35] The authors make use of the fact that Au_4L_4 was the most abundant ion species within fragments of gold NPs. Such Au_4L_4 ions should be either desorbed directly from the NPs' surface or formed from the rearrangements of the surface staple motifs. Therefore, the distribution of $Au_4L_xL'_{(4-x)}$ of the binary ligand shells reflects the arrangement of the two ligands on the NP surfaces. For example, for ligand

DOI: 10.1021/acs.accounts.7b00165
Acc. Chem. Res. 2017, 50, 1911−1919

shells with a random morphology, the distribution of each fragment would follow a binomial distribution: the higher the degree of phase separation, the larger the deviation from binomial distribution. A systematic study of various ligand pairs, summarized in Figure 5, was performed on NPs with both hydrophobic and hydrophilic ligand shells. This method shows that two NPs made by different synthetic procedures exhibit a different degree of phase separation despite having the same ligand ratio. Recently, the same method has been used to characterize mixed ligand coated silver NPs.[36] In combination with computer simulations, it was demonstrated that such technique could provide quantitative information on the size of phase separation domains.[37]

3.5. UV−Vis

The surface plasmon resonance (SPR) peak of a gold NP is sensitive to local dielectric medium and electronic interaction between the free electron cloud inside the gold core and the ligand shell. Vilain et al. synthesized gold NPs initially covered with diphenylphosphinine. Partial replacement of the shell is achieved by ligand exchange with various thiols. The obtained NPs displayed a strong blue shift that depended on the quantity of phosphinine replaced. It was reasoned that the shift was due to the ligand shell having a Janus structure.[38]

3.6. Electron Spin Resonance (EPR)

The advantage of using EPR for NP characterization is that it offers a sensitive detection of free radicals such as thiolated nitroxides that can be incorporated as part of the mixed ligand shell. Molecular conformation state and lateral mobility of the thiolated free-radical, for instance, on the surface of gold NPs could be studied.[39,40]

Gentilini et al. used a free radical molecule (dialkyl nitroxide) as a reporter for the patchiness of the mixed ligand shell.[41] Particles with the ligand shell made of perfluoroalkyl (F8-TEG) and alkyl amphiphilic (C8-TEG) thiols were analyzed. Dialkyl nitroxide partitions almost exclusively close to the fluorinated ligands within the ligand shell, and has EPR signals that are sensitive to local polarity. It was found that the EPR signal of the NPs was practically identical to that generated by fluorinated homoligand NPs, thus indicating the presence of patches in the ligand shell. Only particles with a ligand shell that strongly adsorbs the probe and with a marked difference in the wettability of the patches can be studied by this approach. The spatial resolution of this approach remains undetermined.

3.7. Adsorption-Based Fluorescence Spectroscopy or SERS

The arrangement of thiol molecules within the ligand shell can also be indirectly inferred from its absorption capacity to absorb an analyte. Bonomi et al. studied the adsorption of a charged analyte ATP (adenosine triphosphate) onto gold NPs coated with a mixture of cation terminated thiols (such as those with TACN·Zn^{II} triazacyclononane or trimethylamine headgroups) and inert TEG triethylene glycol-terminated thiols.[42] By varying the amount of the former in the ligand shell, it was shown by a fluorescence titration that the saturation amount of ATP on the ligand shell had a nonlinear, bell-curved trend with a maximum at an intermediate ligand ratio (in between 0.5 and 0.7). Because the multiply charged ATP can interact with several of the cation terminated thiols simultaneously, it can be used to assess the morphology of the ligand shell. A titration experiment in which monoligand-coated NPs was mixed was done as a control and resulted in a linear horizontal trend. This result confirms that the ligand shell of the mixed ligand coated NP is not completely demixed as the Janus morphology. Instead, with the help of simulation it was demonstrated that at the intermediate ligand ratios the charged ligands formed patchy domains that are both large enough to promote maximum binding and spaced just far apart enough by the inter TEG thiols to minimize electrostatic repulsion. Likewise, Stewart et al. used silver NPs coated with pentanethiol and negatively charged mercaptopropanesulfonic acid and observed a markedly saturated absorption of a positive SERS-active analyte ZnTMpyP at only at the ligand shell composition 1:1.[43] In consideration of ligand clustering geometry, it was suggested that clustered domains of both ligands were formed. This arrangement allows an incoming ZnTMpyP to find at least one negatively charged ligand on any part of the NP, hence promoting most efficient binding.

4. SIMULATIONS

A large body of theoretical work has established simulations as a tool to characterize ligand coated gold NPs. Atomistic molecular dynamics (MD) and dissipative particle dynamics (DPD) have reproduced stripelike patterns initially observed in our group for certain binary mixtures of thiolated molecules on gold NPs.[44,45] Singh et al. discovered that the gain of conformational entropy of longer or bulkier molecules at molecular interfaces drives the formation of striped domains, resulting in the system with overall lower free energy than that of complete phase separation.[44] Recently, Ge et al. have used atomistic discrete MD to confirm the existence of striped domains on gold nanoparticle surfaces.[46] Several MD simulations with explicit solvents starting at three different initial configurations (random, striped, and Janus) were performed and led to different final morphologies, suggesting the presence of kinetically trapped states (in agreement with the MS results discussed above). Fetisov et al. performed configurational-bias Monte Carlo simulations in order to establish thermodynamic equilibrium morphologies of various binary thiolated molecules on gold NPs and obtained indeed different degrees of phase separations.[47] In a notable case where hexanethiol and tetradecanethiol molecules were considered, the binary mixture yields the Janus morphology as a final state. The striped morphology is only transient before such a final structure is achieved.

Computer simulations have become an indispensable part of NP characterization. Self-consistent mean field theory has been successfully performed to interpretation of MALDI-TOF data of mixed ligand coated silver NPs.[36,37] Pasquato's group has studied patchy morphologies of water-soluble gold NPs coated with a mixture F- and H- amphiphilic thiolated molecules by ESR and NMR.[28,48] To learn about the mechanism of the molecular separation, the group developed a multiscale simulation approach in which a fully atomistic MD incorporated with explicit presence of water was performed first. The obtained structure and energetics at molecular level were then fed into a dissipative particle dynamics (DPD) mesoscale simulation that explained satisfactorily all the molecular phase-separation states occurring in the ligand shells. We and other groups have also explored the combination of simulation with experimental studies utilizing techniques such as NMR, STM, SANS and found quite reasonable agreement between the two.[12,28,44,45,49]

DOI: 10.1021/acs.accounts.7b00165
Acc. Chem. Res. 2017, 50, 1911−1919

5. PERSPECTVE

At present, there is no method or a combination of several methods that allows us to easily and readily characterize the ligand shell morphology of NPs. Microscopy techniques that have been developed (STM and AFM) or those under development (such as TEM) only characterize a few particles and have complex sample preparation and image interpretation requirements. Moreover, while the microscopy techniques are suitable for a detection of a morphology (e.g., stripe or Janus), they are weak in determining its absence. All microscopy techniques developed to date only produce 2D projections of the 3D object in study, which is another obvious limitation. Spectroscopy techniques on the other hand can be used to characterize the whole ensemble of particles in bulk which is their main advantage. However, presently they have two limitations. The first stems directly from their strength. That is, if an ensemble contains too large variations (in particle size, shape, ligand shell composition, and/or morphology), the resulting spectroscopy measurement will be difficult to interpret or lead to wrong conclusion; hence, uniform samples are required. Unfortunately, uniformity in ligand shell morphology is not simple to achieve if there is no measurement that can establish it. At present, it can only be inferred through property measurements. The second limitation of all the presented spectroscopy measurements with the exception of SANS is that they can only determine if the ligand shell morphology is a part of a class (random, Janus, or patchy) but cannot determine the detailed characteristics of the morphology (e.g., whether the patchy particles are striped or have an arrangement of rounded patches). Simulations appear to be a powerful tool in the field but at present they too are limited to an intrinsically homogeneous sample as they are typically focused on a single particle.

We believe that in order to effectively characterize the morphology of the ligand shell of NPs in the future, effective combination of methods will have to be developed. For example, having quantitative comparisons between SANS model and the residues distribution obtained by mass spectroscopy would be a powerful combination. An approach to quantitatively compare a number of STM images to a SANS model and from it derive a score of the homogeneity of the sample would equally represent a major step forward. At present, some of these approaches are possible only by comparing one experimental technique with simulations. The main stumbling block in developing quantitative comparisons between techniques is the different requirement that each technique has on the sample. For example, STM requires ligands of different length, or more precisely, electronic structure). This affects the nanoparticle synthesis, leading to polydispersed samples that in turn cannot be analyzed by SANS. We have not yet been able to achieve monodisperse particles (i.e., analyzed with SANS) that have a good efficiency in producing Au_4L_4 residues in MS decomposition. Once these limitations are lifted, the field will majorly progress.

All the techniques mentioned in this Account do not cope well with the dynamics of the change of domain structure. In fact, they have not yet been successfully used for following the change of the shell structure; for example, when NPs interact with biological entities or in a catalytic reaction. In such cases, in principle, new methods will have to be developed to selectively resolve NPs against the complex environment.

AUTHOR INFORMATION

Corresponding Author

*E-mail: francesco.stellacci@epfl.ch.

ORCID

Francesco Stellacci: 0000-0003-4635-6080

Author Contributions

†Q.O. and Z.L. contributed equally.

Funding

The authors acknowledge support from the Swiss National Foundation and The EU project Nanofacturing.

Notes

The authors declare no competing financial interest.

Biographies

Quy Ong received his Ph.D. from Purdue University. Currently, he is a senior researcher under the supervision of Prof. Stellacci in the Institute of Materials (IMX) at EPFL.

Zhi Luo is currently a Ph.D. candidate in the IMX at EPFL under the supervision of Prof. Stellacci. He received his B.S. degree from Tsinghua University.

Francesco Stellacci graduated from the Politecnico di Milano and was a postdoc at the University of Arizona. He was professor in the Department of Materials Science and Engineering at MIT. In 2010, he moved as a full professor to EPFL where he holds the Constellium chair in the IMX.

ACKNOWLEDGMENTS

We thank Dr. Matej Janecek for helpful discussion and proofreading of our manuscript.

REFERENCES

(1) Zhao, P.; Li, N.; Astruc, D. State of the art in gold nanoparticle synthesis. *Coord. Chem. Rev.* **2013**, *257*, 638−665.

(2) Daniel, M.-C.; Astruc, D. Gold Nanoparticles: Assembly, Supramolecular Chemistry, Quantum-Size-Related Properties, and Applications toward Biology, Catalysis, and Nanotechnology. *Chem. Rev.* **2004**, *104*, 293−346.

(3) Dreaden, E. C.; Alkilany, A. M.; Huang, X.; Murphy, C. J.; El-Sayed, M. A. The golden age: gold nanoparticles for biomedicine. *Chem. Soc. Rev.* **2012**, *41*, 2740−2779.

(4) Silvera Batista, C. A.; Larson, R. G.; Kotov, N. A. Nonadditivity of nanoparticle interactions. *Science* **2015**, *350*, 1242477.

(5) Kuna, J. J.; Voïtchovsky, K.; Singh, C.; Jiang, H.; Mwenifumbo, S.; Ghorai, P. K.; Stevens, M. M.; Glotzer, S. C.; Stellacci, F. The effect of nanometre-scale structure on interfacial energy. *Nat. Mater.* **2009**, *8*, 837−842.

(6) Centrone, A.; Penzo, E.; Sharma, M.; Myerson, J. W.; Jackson, A. M.; Marzari, N.; Stellacci, F. The role of nanostructure in the wetting behavior of mixed-monolayer-protected metal nanoparticles. *Proc. Natl. Acad. Sci. U. S. A.* **2008**, *105*, 9886−9891.

(7) Hung, A.; Mwenifumbo, S.; Mager, M.; Kuna, J. J.; Stellacci, F.; Yarovsky, I.; Stevens, M. M. Ordering Surfaces on the Nanoscale: Implications for Protein Adsorption. *J. Am. Chem. Soc.* **2011**, *133*, 1438−1450.

(8) Jackson, A. M.; Myerson, J. W.; Stellacci, F. Spontaneous assembly of subnanometre-ordered domains in the ligand shell of monolayer-protected nanoparticles. *Nat. Mater.* **2004**, *3*, 330−336.

(9) Verma, A.; Uzun, O.; Hu, Y. H.; Hu, Y.; Han, H. S.; Watson, N.; Chen, S. L.; Irvine, D. J.; Stellacci, F. Surface-structure-regulated cell-membrane penetration by monolayer-protected nanoparticles. *Nat. Mater.* **2008**, *7*, 588−595.

DOI: 10.1021/acs.accounts.7b00165
Acc. Chem. Res. 2017, 50, 1911−1919

(10) Ghosh, A.; Basak, S.; Wunsch, B. H.; Kumar, R.; Stellacci, F. Effect of Composition on the Catalytic Properties of Mixed-Ligand-Coated Gold Nanoparticles. *Angew. Chem., Int. Ed.* **2011**, *50*, 7900−7905.
(11) Cho, E. S.; Kim, J.; Tejerina, B.; Hermans, T. M.; Jiang, H.; Nakanishi, H.; Yu, M.; Patashinski, A. Z.; Glotzer, S. C.; Stellacci, F.; Grzybowski, B. A. Ultrasensitive detection of toxic cations through changes in the tunnelling current across films of striped nanoparticles. *Nat. Mater.* **2012**, *11*, 978−985.
(12) Moglianetti, M.; Ong, Q. K.; Reguera, J.; Harkness, K. M.; Mameli, M.; Radulescu, A.; Kohlbrecher, J.; Jud, C.; Svergun, D. I.; Stellacci, F. Scanning tunneling microscopy and small angle neutron scattering study of mixed monolayer protected gold nanoparticles in organic solvents. *Chem. Sci.* **2014**, *5*, 1232−1240.
(13) Ong, Q. K.; Reguera, J.; Silva, P. J.; Moglianetti, M.; Harkness, K.; Longobardi, M.; Mali, K. S.; Renner, C.; De Feyter, S.; Stellacci, F. High-Resolution Scanning Tunneling Microscopy Characterization of Mixed Monolayer Protected Gold Nanoparticles. *ACS Nano* **2013**, *7*, 8529−8539.
(14) Stirling, J.; Lekkas, I.; Sweetman, A.; Djuranovic, P.; Guo, Q.; Pauw, B.; Granwehr, J.; Lévy, R.; Moriarty, P. Critical Assessment of the Evidence for Striped Nanoparticles. *PLoS One* **2014**, *9*, e108482.
(15) Cesbron, Y.; Shaw, C. P.; Birchall, J. P.; Free, P.; Levy, R. Stripy Nanoparticles Revisited. *Small* **2012**, *8*, 3714−3719.
(16) Yu, M.; Stellacci, F. Response to ″Stripy Nanoparticles Revisited″. *Small* **2012**, *8*, 3720−3726.
(17) Ong, Q. K.; Stellacci, F. Response to "Critical Assessment of the Evidence for Striped Nanoparticles. *PLoS One* **2015**, *10*, e0135594.
(18) Hu, Y.; Wunsch, B. H.; Sahni, S.; Stellacci, F. Statistical Analysis of Scanning Tunneling Microscopy Images of 'Striped' Mixed Monolayer Protected Gold Nanoparticles. *J. Scanning Probe Microsc.* **2009**, *4*, 24−35.
(19) Jackson, A. M.; Hu, Y.; Silva, P. J.; Stellacci, F. From homoligand- to mixed-ligand-monolayer-protected metal nanoparticles: A scanning tunneling microscopy investigation. *J. Am. Chem. Soc.* **2006**, *128*, 11135−11149.
(20) Biscarini, F.; Ong, Q. K.; Albonetti, C.; Liscio, F.; Longobardi, M.; Mali, K. S.; Ciesielski, A.; Reguera, J.; Renner, C.; De Feyter, S.; Samorì, P.; Stellacci, F. Quantitative Analysis of Scanning Tunneling Microscopy Images of Mixed-Ligand-Functionalized Nanoparticles. *Langmuir* **2013**, *29*, 13723−13734.
(21) Ong, Q. K.; Zhao, S.; Reguera, J.; Biscarini, F.; Stellacci, F. Comparative STM studies of mixed ligand monolayers on gold nanoparticles in air and in 1-phenyloctane. *Chem. Commun.* **2014**, *50*, 10456−10459.
(22) Wang, Y.; Zeiri, O.; Neyman, A.; Stellacci, F.; Weinstock, I. A. Nucleation and Island Growth of Alkanethiolate Ligand Domains on Gold Nanoparticles. *ACS Nano* **2012**, *6*, 629−640.
(23) Lee, Z.; Jeon, K. J.; Dato, A.; Erni, R.; Richardson, T. J.; Frenklach, M.; Radmilovic, V. Direct Imaging of Soft-Hard Interfaces Enabled by Graphene. *Nano Lett.* **2009**, *9*, 3365.
(24) Yang, J. A.; Murphy, C. J. Evidence for Patchy Lipid Layers on Gold Nanoparticle Surfaces. *Langmuir* **2012**, *28*, 5404−5416.
(25) Meena, S. K.; Goldmann, C.; Nassoko, D.; Seydou, M.; Marchandier, T.; Moldovan, S.; Ersen, O.; Ribot, F.; Chanéac, C.; Sanchez, C.; Portehault, D.; Tielens, F.; Sulpizi, M. Nanophase Segregation of Self-Assembled Monolayers on Gold Nanoparticles. *ACS Nano* **2017**, *11*, 7371−7381.
(26) Marbella, L. E.; Millstone, J. E. NMR Techniques for Noble Metal Nanoparticles. *Chem. Mater.* **2015**, *27*, 2721−2739.
(27) Liu, X.; Yu, M.; Kim, H.; Mameli, M.; Stellacci, F. Determination of monolayer-protected gold nanoparticle ligand-shell morphology using NMR. *Nat. Commun.* **2012**, *3*, 1182.
(28) Şologan, M.; Marson, D.; Polizzi, S.; Pengo, P.; Boccardo, S.; Pricl, S.; Posocco, P.; Pasquato, L. Patchy and Janus Nanoparticles by Self-Organization of Mixtures of Fluorinated and Hydrogenated Alkanethiolates on the Surface of a Gold Core. *ACS Nano* **2016**, *10*, 9316−9325.
(29) Guarino, G.; Rastrelli, F.; Scrimin, P.; Mancin, F. Lanthanide-Based NMR: A Tool To Investigate Component Distribution in Mixed-Monolayer-Protected Nanoparticles. *J. Am. Chem. Soc.* **2012**, *134*, 7200−7203.
(30) Salorinne, K.; Malola, S.; Wong, O. A.; Rithner, C. D.; Chen, X.; Ackerson, C. J.; Häkkinen, H. Conformation and dynamics of the ligand shell of a water-soluble Au102 nanoparticle. *Nat. Commun.* **2016**, *7*, 10401.
(31) Hostetler, M. J.; Stokes, J. J.; Murray, R. W. Infrared Spectroscopy of Three-Dimensional Self-Assembled Monolayers: N-Alkanethiolate Monolayers on Gold Cluster Compounds. *Langmuir* **1996**, *12*, 3604−3612.
(32) Centrone, A.; Hu, Y.; Jackson, A. M.; Zerbi, G.; Stellacci, F. Phase separation on mixed-monolayer-protected metal nanoparticles: A study by infrared spectroscopy and scanning tunneling microscopy. *Small* **2007**, *3*, 814−817.
(33) Harkness, K. M.; Cliffel, D. E.; McLean, J. A. Characterization of thiolate-protected gold nanoparticles by mass spectrometry. *Analyst* **2010**, *135*, 868−874.
(34) Yan, B.; Zhu, Z.-J.; Miranda, O. R.; Chompoosor, A.; Rotello, V. M.; Vachet, R. W. Laser desorption/ionization mass spectrometry analysis of monolayer-protected gold nanoparticles. *Anal. Bioanal. Chem.* **2010**, *396*, 1025−1035.
(35) Harkness, K. M.; Balinski, A.; McLean, J. A.; Cliffel, D. E. Nanoscale Phase Segregation of Mixed Thiolates on Gold Nanoparticles. *Angew. Chem., Int. Ed.* **2011**, *50*, 10554−10559.
(36) Farrell, Z.; Merz, S.; Seager, J.; Dunn, C.; Egorov, S.; Green, D. L. Development of Experiment and Theory to Detect and Predict Ligand Phase Separation on Silver Nanoparticles. *Angew. Chem., Int. Ed.* **2015**, *54*, 6479−82.
(37) Merz, S. N.; Farrell, Z. J.; Dunn, C. J.; Swanson, R. J.; Egorov, S. A.; Green, D. L. Theoretical and Experimental Investigation of Microphase Separation in Mixed Thiol Monolayers on Silver Nanoparticles. *ACS Nano* **2016**, *10*, 9871−9878.
(38) Vilain, C.; Goettmann, F.; Moores, A.; Le Floch, P.; Sanchez, C. Study of metal nanoparticles stabilised by mixed ligand shell: a striking blue shift of the surface-plasmon band evidencing the formation of Janus nanoparticles. *J. Mater. Chem.* **2007**, *17*, 3509−3514.
(39) Ionita, P.; Volkov, A.; Jeschke, G.; Chechik, V. Lateral Diffusion of Thiol Ligands on the Surface of Au Nanoparticles: An Electron Paramagnetic Resonance Study. *Anal. Chem.* **2008**, *80*, 95−106.
(40) Ionita, P.; Wolowska, J.; Chechik, V.; Caragheorgheopol, A. Ligand Dynamics in Spin-Labeled Au Nanoparticles. *J. Phys. Chem. C* **2007**, *111*, 16717−16723.
(41) Gentilini, C.; Franchi, P.; Mileo, E.; Polizzi, S.; Lucarini, M.; Pasquato, L. Formation of Patches on 3D SAMs Driven by Thiols with Immiscible Chains Observed by ESR Spectroscopy. *Angew. Chem., Int. Ed.* **2009**, *48*, 3060−3064.
(42) Bonomi, R.; Cazzolaro, A.; Prins, L. J. Assessment of the morphology of mixed SAMs on Au nanoparticles using a fluorescent probe. *Chem. Commun.* **2011**, *47*, 445−447.
(43) Stewart, A.; Zheng, S.; McCourt, M. R.; Bell, S. E. J. Controlling Assembly of Mixed Thiol Monolayers on Silver Nanoparticles to Tune Their Surface Properties. *ACS Nano* **2012**, *6*, 3718−3726.
(44) Singh, C.; Ghorai, P.; Horsch, M.; Jackson, A.; Larson, R.; Stellacci, F.; Glotzer, S. Entropy-Mediated Patterning of Surfactant-Coated Nanoparticles and Surfaces. *Phys. Rev. Lett.* **2007**, *99*, 226106.
(45) Ghorai, P. K.; Glotzer, S. C. Atomistic Simulation Study of Striped Phase Separation in Mixed-Ligand Self-Assembled Monolayer Coated Nanoparticles. *J. Phys. Chem. C* **2010**, *114*, 19182−19187.
(46) Ge, X.; Ke, P. C.; Davis, T. P.; Ding, F. A Thermodynamics Model for the Emergence of a Stripe-like Binary SAM on a Nanoparticle Surface. *Small* **2015**, *11*, 4894−4899.
(47) Fetisov, E. O.; Siepmann, J. I. Structure and Phase Behavior of Mixed Self-Assembled Alkanethiolate Monolayers on Gold Nanoparticles: A Monte Carlo Study. *J. Phys. Chem. B* **2016**, *120*, 1972−1978.
(48) Posocco, P.; Gentilini, C.; Bidoggia, S.; Pace, A.; Franchi, P.; Lucarini, M.; Fermeglia, M.; Pricl, S.; Pasquato, L. Self-Organization of

DOI: 10.1021/acs.accounts.7b00165
Acc. Chem. Res. 2017, 50, 1911−1919

Mixtures of Fluorocarbon and Hydrocarbon Amphiphilic Thiolates on the Surface of Gold Nanoparticles. *ACS Nano* **2012**, *6*, 7243−7253.
(49) Van Lehn, R. C.; Alexander-Katz, A. Structure of Mixed-Monolayer-Protected Nanoparticles in Aqueous Salt Solution from Atomistic Molecular Dynamics Simulations. *J. Phys. Chem. C* **2013**, *117*, 20104−20115.

DOI: 10.1021/acs.accounts.7b00165
Acc. Chem. Res. 2017, 50, 1911−1919